



CORROSION INHIBITION OF STEEL BY PRICKLY PEAR: EXTRACTION, CHARACTERIZATION AND ELECTROCHEMICAL STUDIES

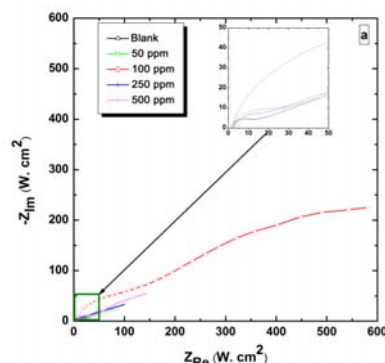
Imen ABIDLI,^{a,*} Nebil SOUSSI^a and X. Ramón NÓVOA^b

^aUniversity of Tunis El Manar, Preparatory Institute for Engineering Studies, BP 244 El Manar II, 2092 El Manar, Tunis, Tunisia

^bUniversity of Vigo, School of Industrial Engineering, E-36310-Vigo, Spain

Received October 5, 2019

Aqueous and Methanolic extracts of Prickly Pear was tested as a corrosion inhibitor for mild steel using electrochemical impedance spectroscopy (EIS) in two different media. Impedance measurements showed that there are two phenomena in the inhibition process. The obtained results show that this plant extract could serve as an effective inhibitor for corrosion of steel in NaOH solutions with different NaCl content. The aqueous extract obtained gives inhibition around 96.9% in 0.1 M NaOH solution and the methanolic extract provided about 88.3% inhibition efficiency in 0.1 M NaOH+0.5 M NaCl solution. The EIS experimental data show frequency dispersion and therefore a modeling element with frequency dispersion behavior, a constant phase (CPE) has been used.



INTRODUCTION

The corrosion of mild steel has received a considerable amount of attention because of its industrial concern. The study of corrosion inhibition of mild steel in acidic media is one of the challenging topics of current research in various industries involving chemical cleaning, descaling, pickling, etc.¹⁻⁵ The use of inhibitors is also one of the main methods for protection of steel against corrosion in alkaline environments as concrete, where organic⁶ and inorganic compounds^{7,8} are employed.

Recently, natural compounds have been employed as inhibitors in order to develop new solutions compatible with the sustainable environment concept. The use of these natural products, such as those extracted from leaves or several authors⁹⁻¹⁴ have reported seeds, as corrosion inhibitors. Prickly Pear is a common plant from Tunisia. It is currently employed as medical treatment against aches. Prickly

Pear is found to contain carbohydrates, protein, lipids, amino acids, vitamins, minerals, polyphenols, and betalain pigments.^{15,16} Most of those compounds are potential corrosion inhibitors, specially amino acids² and polyphenols.^{3,4}

This study aims at gaining some insight into the corrosion inhibition of steel in three different alkaline media by aqueous and methanol extracts from Prickly Pear plant.

RESULTS AND DISCUSSION

Open circuit potential

The evolution of the open circuit potential (E_{OCP}) with time for mild steel in different medias without and with Prickly Pear extracts was measured. Before each electrochemical impedance

*Corresponding author: abidliimen@gmail.com or imen.abdili@fst.utm.tn

spectroscopy (EIS) experiments, the electrode was allowed to corrode freely and its open circuit potential (E_{OCP}) was recorded as a function of time up to 180 seconds. After this time a steady state OCP, corresponding to the corrosion potential of the working electrode, was obtained. The above procedures were repeated on 100 ppm of concentration of Prickly Pear methanolic extract and 100 ppm of concentration of Prickly Pear aqueous extract in 0.1 M NaOH+ 0.5 M NaCl and 0.1 M NaOH respectively. The evolution of the open circuit potential (E_{OCP}) with time for mild steel in different medias revealed that the plots showed clear modifications in the E_{OCP} –time behavior due to the presence of Prickly Pear extracts.

Without inhibitor, the electrode of mild steel had an E_{OCP} –0.55 Vvs.SCE and –0.37 Vvs.SCE at $t = 0$ min and at $t = 240$ min, respectively. Therefore, the oxide film is formed over time, the one that covers the surface and performs the anodic displacement of the potential. When inhibitor was present in the electrolyte solution at $t = 160$ min, a positive shift in E_{OCP} was changed from –0.36 Vvs.SCE in the uninhibited solution to –0.3 Vvs.SCE. At $t = 240$ min, the electrode of mild steel had an E_{OCP} –0.28 Vvs.SCE. The positive shift in E_{OCP} indicated that the molecules inhibited the anodic corrosion of mild steel.

Without inhibitor, the electrode of mild steel had an E_{OCP} –0.39 Vvs.SCE and –0.5 Vvs.SCE at $t = 0$ min and at $t = 140$ min, respectively. This cathodic displacement is due to the corrosion of the surface incurring by the Cl^- ions attack. From $t = 160$ min to $t = 240$ min, the electrode of mild steel had an E_{OCP} –0.45 Vvs.SCE and –0.48 Vvs.SCE. An anodic displacement was observed and decrease towards the cathodic values. In the employed chloride environment, a magnetite-rich passive layer develops at the metallic surface^{22,23} that tends to dissolve locally in the presence of chlorides²⁴. When inhibitor was present in the electrolyte solution at $t = 160$ min, a positive shift in E_{OCP} was changed from –0.45 Vvs.SCE in the uninhibited solution to –0.35 Vvs.SCE. At $t = 240$ min, the electrode of mild steel had an E_{OCP} –0.28 Vvs.SCE. The positive shift in E_{OCP} indicated that the presence of inhibitor is expected to affect the building up of the passive layer, and passivity breakdown.

Electrochemical impedance spectroscopy

The impedance method has been used to get the information about kinetics of the electrode

processes and, simultaneously, about the surface properties of the investigated systems.

The method is widely used for investigation of the corrosion inhibition processes.^{25,26}

Fig. 2 shows the Nyquist and Bode-phase plots for mild steel in 0.1 M NaOH+ 0.5 M NaCl and in 0.1 M NaOH solutions in absence and presence of various concentrations of Prickly Pear methanolic and aqueous extracts, respectively at 25°. The impedance spectra obtained for the corrosion of studied mild steel in 0.1 M NaOH+ 0.5 M NaCl and in 0.1 M NaOH solutions with and without inhibitor consist of two capacitive loops (two well-defined time-constants in the phase format; Fig. 2b and Fig. 2d). The high-frequency (HF) loop, the smaller one, can be attributed to the film formation at the steel surface while the low-frequency (LF) loop, the larger one, can be attributed to the charge transfer reaction. Fig. 2a and Fig. 2c exhibit two single depressed semicircles. The diameter of the semicircle at high frequency reached the maximum at 100 ppm of Prickly Pear methanolic extract. The high frequency time constant corresponds to the charge transfer resistance in parallel to the double layer capacitance. The low frequency tail can be either attributed to oxygen diffusion or redox transformations (Fe^{3+}/Fe^{2+}) at the electrode surface, or both phenomena with some degree of overlapping. According to the shape of the experimental EIS spectra, the low frequency tail approaches Warburg-type diffusion only for the blank solution and that containing 50 ppm inhibitor (all spectra fitted by the same model). For higher inhibitor concentrations, the charge transfer resistance increases (corrosion rate decreases) so that oxygen transport no longer controls the reaction rate and the low frequency time constant can be associated to redox transformations exclusively.

Excellent fit with the equivalent circuit model $R_e (C_{dl}R_{ct})$ was obtained for all experimental data, depicted in Fig. 3a. In this equivalent circuit, R_e is the electrolyte resistance, R_{ct} is the charge transfer resistance and CPE is substituted for the capacitive element to give a more accurate fit, as most capacitive loops are depressed semicircles rather than regular semicircles. As an example, the Nyquist plots of experimental data (in the presence of 100 ppm Prickly Pear methanolic extract) and simulated are presented in Fig. 3b. The deviation of semicircles from perfect circular shape is often referred to the frequency dispersion of interfacial impedance^{27,28}. This behavior is usually attributed to the inhomogeneity of the metal surface arising from surface roughness or interfacial phenomena^{29,30} which is typical for solid metal electrodes.³¹

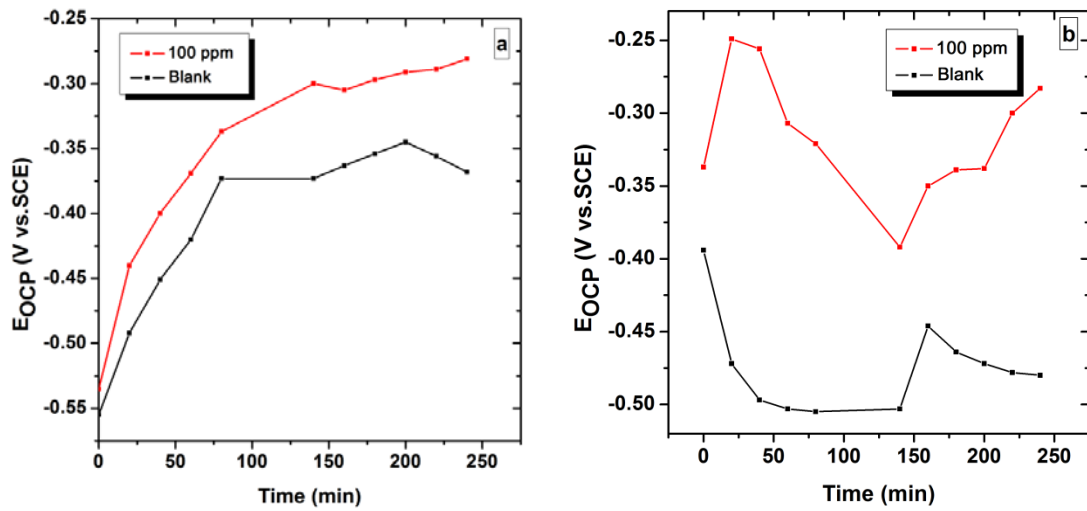


Fig. 1 – Open-circuit potential – time variation of carbon steel in: **a)** 0.1 M NaOH solution without and with Prickly Pear aqueous extract **b)** 0.1 M NaOH + 0.5 M NaCl solution without and with Prickly Pear methanolic extract.

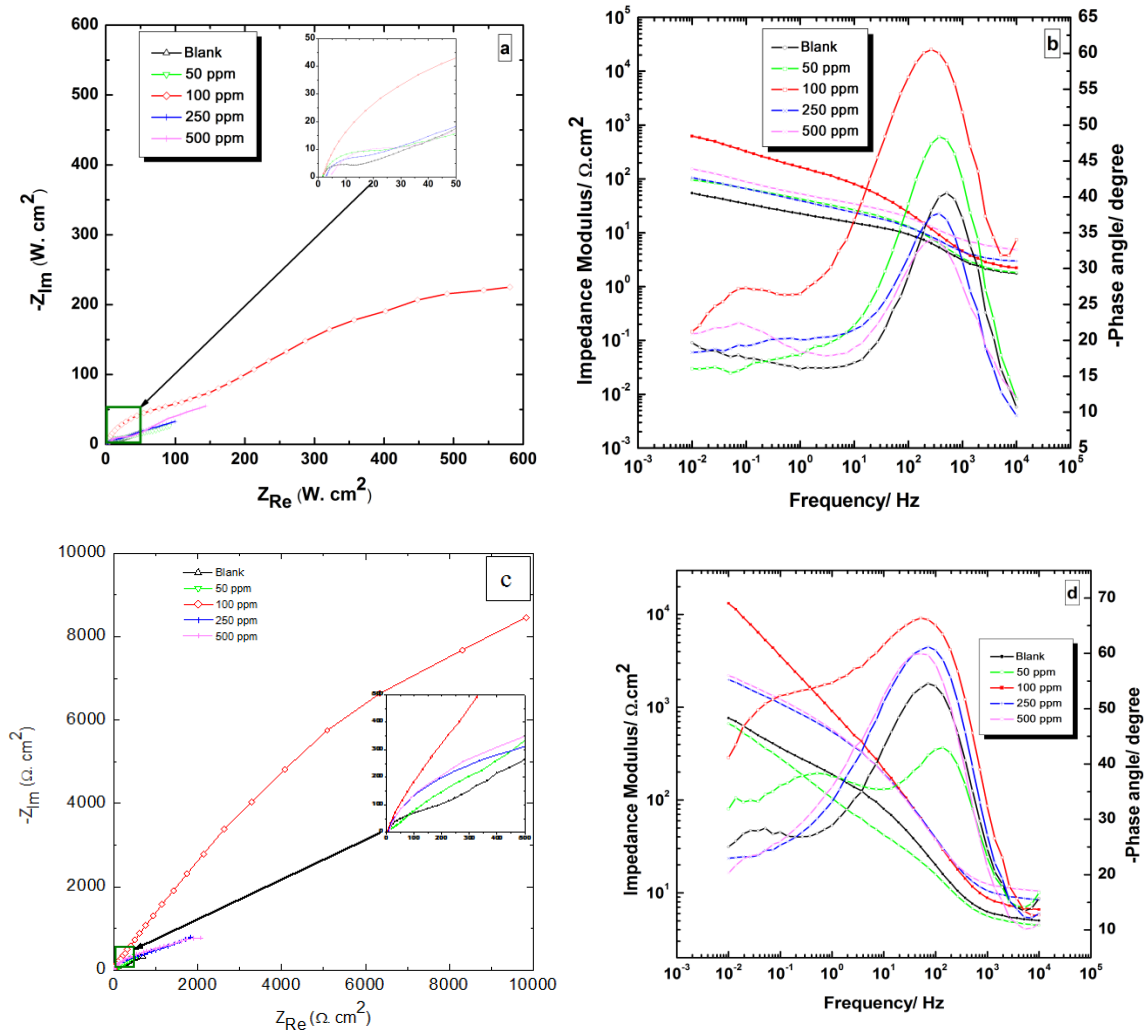


Fig. 2 – Electrochemical impedance spectra of carbon steel **a)** Nyquist plot in 0.1 M NaOH + 0.5 M NaCl solution without and with Prickly Pear methanolic extract **b)** Bode-phase angle plots in 0.1 M NaOH + 0.5 M NaCl solution without and with Prickly Pear methanolic extract **c)** Nyquist plot in 0.1 M NaOH solution without and with Prickly Pear aqueous extract **d)** Bode phase angle plot in 0.1 M NaOH solution without and with Prickly Pear aqueous extract.

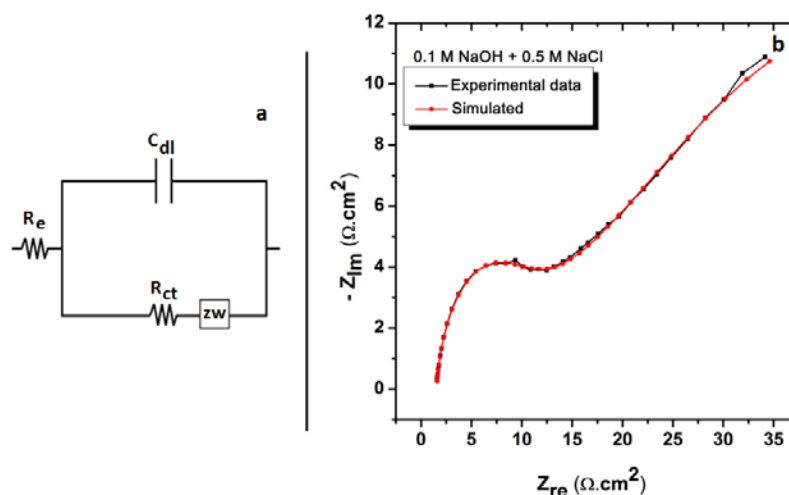


Fig. 3 – **a**) Equivalent circuits of electrochemical impedance spectra integrating the effect of diffusion of a Warburg impedance without and with inhibitor **b**) Experimental and computer fitted results of Nyquist plot for mild steel in 0.1 M NaOH + 0.5 M NaCl solution containing 100 ppm of Prickly Pear methanolic extract.

In this behavior of solid electrodes, the parallel network: charge transfer resistance-double layer capacitance is established where an inhibitor is present. For the description of a frequency independent phase shift between an applied ac potential and its current response, a constant phase element (CPE) is used which is defined in impedance representation as in Eq. (1).³¹

$$Z_{CPE} = \frac{1}{Q(j\omega)^\alpha} \quad (1)$$

where Q is the magnitude of CPE, α is the CPE exponent; ω is the angular frequency in rad s^{-1} ($\omega = 2\pi f$ when f is the frequency in Hz); $j = (-1)^{1/2}$ is an imaginary number, and Z_{CPE} , impedance of CPE. The CPE, which is considered as a surface irregularity of the electrode, causes a greater depression in Nyquist semicircle diagram, where the metal-solution interface acts as a capacitor with irregular surface. If the electrode surface is homogeneous and plane, the exponential value (α) becomes equal to 1 and the metal-solution interface acts as a capacitor with regular surface.³² C_{dl} values derived from CPE parameters according to Eq. (2) can be calculated:³³

$$C_{dl} = Q_{dl}(2\pi f_{max})^{\alpha-1} \quad (2)$$

where f_{max} represents the frequency at which imaginary value reaches a maximum on the Nyquist plot.

Various parameters such as the charge transfer resistance R_{ct} , double layer capacitance C_{dl} and percentage inhibition efficiency were calculated from equivalent circuit model and listed in Table 1. The polarization resistance (R_p) was calculated by:

$$R_p = R_e + R_{ct} \quad (3)$$

The values of IE % are calculated using the following equation:³⁴

$$IE (\%) = \frac{R_{ct}(inh) - R_{ct}}{R_{ct}(inh)} * 100 \quad (4)$$

where R_{ct} and $R_{ct}(inh)$ are charge transfer resistances in the absence and the presence of inhibitor. Inspection of data in Table 1 shows clearly that R_{ct} and C_{dl} values have opposite trend at the whole concentration range (R_{ct} increases and C_{dl} decreases with inhibitor concentration). The double-layer capacitance reduced by increasing the concentration is in agreement with partial coverage of the surface by an insulating layer of low dielectric constant,⁵ as that provided by the inhibitor. This situation according to the Helmholtz model was the result of an increase in the thickness of the electrical double layer or/an assigned to a decrease in local dielectric constant.³⁵ The phase angle at high frequencies provides a general idea of corrosion inhibition performance. The more negative the phase angle, the more capacitive the electrochemical behavior (Fig. 2b and Fig. 2d). Charge-transfer resistance increment raises the current tendency to pass through the capacitor in the circuit. Also, increment of the phase angle at relaxation frequency in presence of inhibitors indicates the increase of capacitive response. Such a phenomenon could be attributed to high corrosion inhibition activity of inhibitor. We noted also that the C_{dl} value does not reach a minimum value at 100 ppm of concentration. It is clear, according to the Figure 4, that the adsorption is monolayer for the concentrations 50 and 100 ppm.

On the other hand, the adsorption is multi-layered for the high concentrations of 250 and 500 ppm. Since there is a multilayer deposition on the surface, the continuous decreasing of capacitance arrived at minimum values for the 250 and 500 ppm concentrations but the resistance does not increase. This reduction in resistance is due to the local fractures of the multilayers, which generates the pores at the level of these fractures. From where, the electrolyte penetrates into these pores and the resistance makes an ohmic drop.

Scanning electron microscopy

SEM micrographs obtained from steel surface specimens immersion in 0.1 M NaOH + 0.5 M NaCl solution for 6 h in the absence and presence of 100 ppm of prickly pear methanolic extract are shown in Fig. 5a-d. The Fig. 5a, which is the micrograph of the mild steel polished surface, showed polished mild steel surface; the polishing stretches were also visible on the surface. Fig. 5b revealed the SEM image of the mild steel surface

exposed to inhibited 0.1 M NaOH + 0.5 M NaCl solution for 6 h in the presence of 100 ppm of prickly pear methanolic extract at 25°C. There are less pits and cracks observed in the micrographs. The surface analysis results suggest higher adsorption of inhibitor on the surface, which support the EIS results. The Fig. 5c, introduced in 0.1 M NaOH + 0.5 M NaCl solution for 6 h in the presence of 100 ppm of prickly pear methanolic extract at 45°C, is rougher with clear pits and cavities. The Fig. 5d, exposed to 0.1 M NaOH + 0.5 M NaCl solution for 6 h in the presence of 100 ppm of prickly pear methanolic extract at 25°C, it can be observed that the mild steel surface was more damage. In other words, the mild steel surface was strongly damaged in the higher temperature. However, it was shown that there was much less damage on the surface of the mild steel and good protective film adsorbed on specimens surface which is responsible for the inhibition of corrosion with prickly pear methanolic extract in 0.1 M NaOH + 0.5 M NaCl solution.

Table 1

Impedance parameters for carbon steel in 0.1 M NaOH in the absence and presence of Prickly Pear aqueous extract and in 0.1 M NaOH + 0.5 M NaCl in the absence and presence of Prickly Pear methanolic extract at 25

System	Re ($\Omega \cdot \text{cm}^2$)	R _{ct} ($\Omega \cdot \text{cm}^2$)	R _p ($\Omega \cdot \text{cm}^2$)	C _{dl} ($\mu\text{F} \cdot \text{cm}^{-2}$)	η (%)
0.1 M NaOH	4.9	8.1	13	114	-
50 ppm	4.5	22.3	26.8	96.7	63.6
100 ppm	6.1	262	268.1	60.2	96.9
250 ppm	8.4	2.8	11.2	29.9	-
500 ppm	10.6	2	12.6	30.6	-
0.1 M NaOH + 0.5 M NaCl	1.7	7	8.7	82.5	-
50 ppm	1.7	9.7	11.4	71.6	28.1
100 ppm	1.7	59.6	61.3	70.4	88.3
250 ppm	2.8	7.49	10.3	64.7	7.1
500 ppm	4.4	23.3	27.7	61.7	70.1

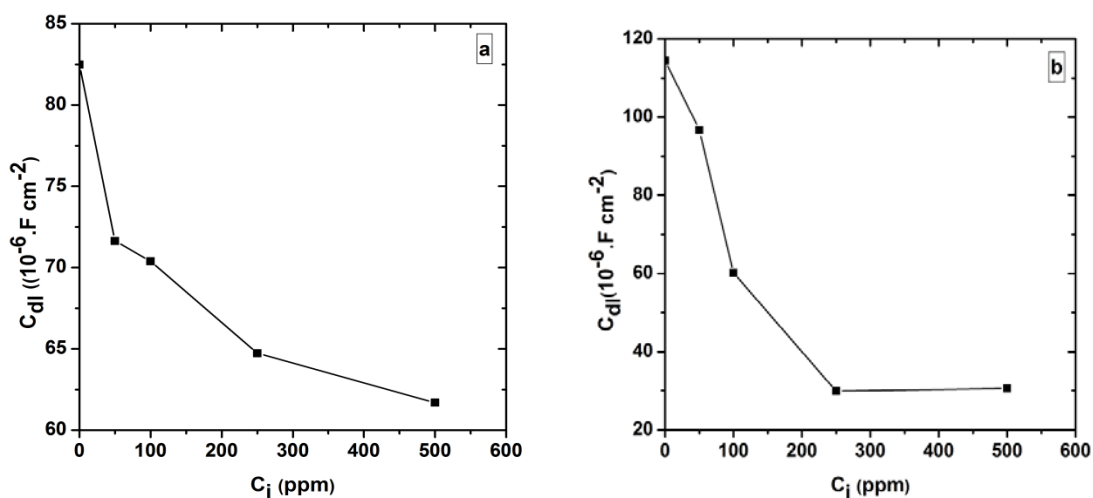


Fig. 4 – Evolution of capacity a) without and with addition of different concentrations of Prackly Pear methanolic extract b) without and with addition of different concentrations of Prackly Pear aqueous extract.

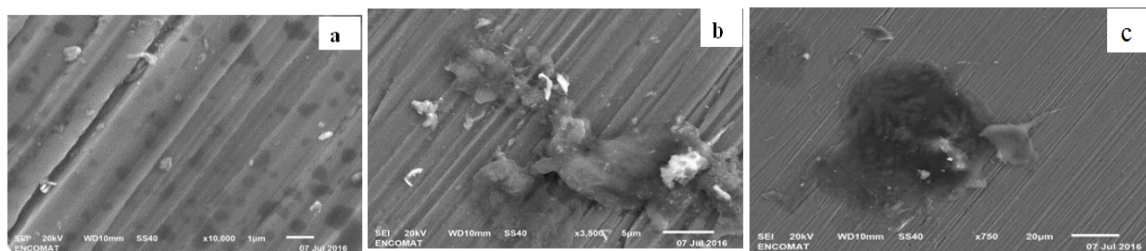


Fig. 5 – SEM micrographs of the mild steel surface: **a)** polished surface **b)** after immersion in 0.1 M NaOH+ 0.5 M NaCl solution for 6 h in the presence of 100 ppm of prickly pear methanolic extract at 25°C **c)** after immersion in 0.1 M NaOH+ 0.5 M NaCl solution for 6 h in the presence of 100 ppm of prickly pear methanolic extract at 45°C.

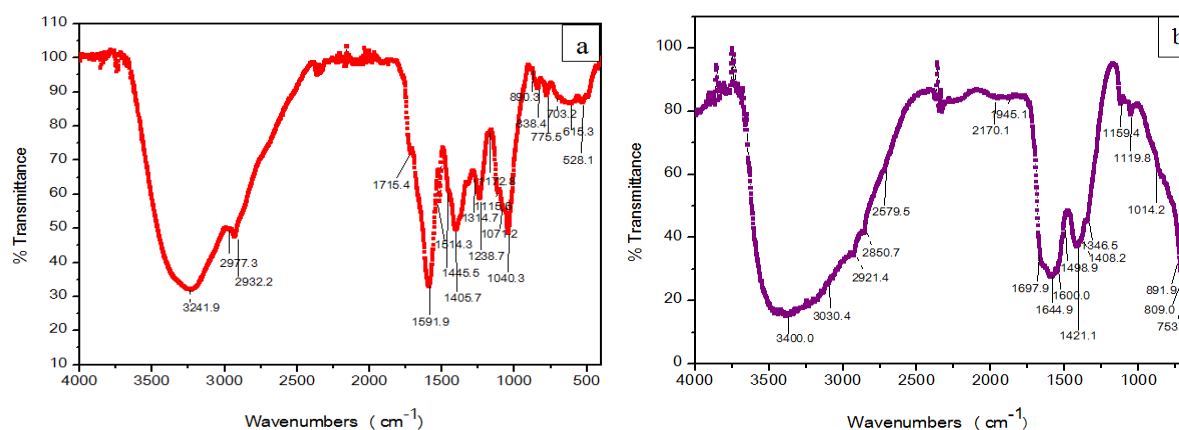


Fig. 6 – FTIR spectra of **a)** Prickly Pear powder of methanolic extract **b)** surface film of the C-steel specimen after 6 H immersion in 0.1M NaOH + 0.5M NaCl containing 100 ppm of Prickly Pear methanolic extract at 25°C.

FT-IR analysis

FTIR is a powerful technique that is always used to determine the type of bonding for organic inhibitors absorbed on the metal surface^{36–38}. Fig. 6a shows the FTIR spectrum of the Prickly Pear powder of methanolic extract. In this sample appear bands at 2800-3000 cm^{-1} that indicate the presence of C-H band. The broadband at 3240-3270 cm^{-1} is attributed to N-H stretching (obligatory) and another around 1600 cm^{-1} corresponds to C = O of N-C = O stretching vibrations, which may indicate the presence of the amide group, but must be confirmed by the presence of N elementary analyzes. Also, the broadband at 3200 cm^{-1} may be provided by the vibration mode of the phenolic OH group, which is also reflected by the bands in the area of 1600 cm^{-1} by the mode of vibration of the C = C of the aromatic cycle, and the bands at 1255-1240 (a little wide, phenolic binding CO), 1170 (phenolic OH) and 835 cm^{-1} (phenolic OH). The bands at 1000-1100 cm^{-1} may be due to stretching vibration modes of the C-O bands in the C-OH group. The band of 1715 cm^{-1} zone is the C = O band, probably the carboxylic acid (COOH). Fig. 6b illustrates the FTIR spectrum of the surface film on

the C-steel specimen after 6 H of immersion in 0.1 M NaOH+0.5 M NaCl containing 100 ppm of Prickly Pear methanolic extract. In the sample, several areas of the surface were measured by the FTIR-microscopy to observe if there is homogeneity according to the possible compound. Using a MCTA detector (mercury cadmium telluride) which is used in measurements of microscopy-FTIR, does not work with frequencies lower than 650 cm^{-1} so that the vibration modes of binding Fe-O of Fe(III) oxides (Fe_2O_3) cannot be observed, such as hematite (540 y 470 cm^{-1}) or maghemite (630 y 430 cm^{-1}) rather than iron oxides II / III as magnetite (Fe_3O_4) (570 and 390 cm^{-1}). A large number of wave shows a very broad band between 2500 y 3700 cm^{-1} which may be provided by a large number of vibration modes of different links between it the O-H bond. As shown in the literature that the band has a maximum absorption at $\approx 3400 \text{ cm}^{-1}$ indicating the presence of polyphenols that they have reacted with the metal, in this case steel. In the region of 1500-1700 cm^{-1} broad band was observed, which may indicate the formation of an amorphous nature of the complex. The band of 1245 cm^{-1} does not appear in Fig. 6b but 1407 cm^{-1} , generally moves at higher wave

number ($1408\text{--}1423\text{ cm}^{-1}$). Several bands are detected which may be due to the presence of various iron oxides groups. The bands around 1018 and 750 cm^{-1} could be due to lepidocrocite bending modes $\text{FeO}(\text{OH})$. The band of $1344\text{--}1350\text{ cm}^{-1}$ may be due to the bending mode of the OH group of a ferric hydroxide $\text{Fe}(\text{OH})_3$. The vibration band of this link would be around 3030 cm^{-1} , and the bands of $1638\text{--}1645\text{ cm}^{-1}$, 890 cm^{-1} and $\approx 800\text{ cm}^{-1}$ could be due to different modes of bending goethite $\text{FeO}(\text{OH})$.

EXPERIMENTAL

Materials and methods

The fruit

Prickly Pear grows, essentially, in the tropical and subtropical regions. It is one of the fewest plants able to adapt to difficult ambient conditions.¹⁷ Prickly Pear grows all throughout Tunisia, in areas characterized by water stress and low soil quality. Fresh Prickly Pearfruits have been used as human food while cladodes have been exploited as livestock forage, essentially during the dry season. In Tunisia, this cactus has been used to prevent soil degradation and to control desertification.¹⁸ The chemical composition of the cactus forage varies with the cultivar, the development stage, the fertilization, the plant population and the cladode order.¹⁹ Nevertheless, the main shared compounds are pectin, mucilage and minerals.²⁰

Extraction procedure

The fruits of the Prickly Pear were harvested during the month of April in the Tunis region. After thoroughly washing to remove adherences, the fruits were cut into small pieces. After that, they were dry ground with a household blender. The resulting sauce was weighed (750g) and was stored in the refrigerator at temperature of $10\text{ }^\circ\text{C}$ until use. To exploit the polar fraction of the Prickly Pear as an inhibitor of corrosion, we conducted two types of extract:

- Aqueous extract. We made macerating 372 g sauce in 0.5 L of water for 16 hours and then made the maceration stirring for 6 hours. The aqueous extract was sieve filtered using successively small pore diameters: 1 mm and 0.080 mm. Filtration was carried out for 24 hours for recovering 450 mL of filtrate having 11.4 g / L concentration.
- Methanolic extract. The same procedure as for the aqueous extract was followed. The concentration of the methanolic extract was 14.6 g / L.

Preparation of the specimens

Mild steel (0.023% P; 0.04% Si; 0.017% Mn; 0.078% C; 0.02% S; 0.002% Mo; Fe balance) specimens of 0.1 cm^2 exposed surface were used for the electrochemical studies. The specimens were polished successively using 400 and 1200 emery papers and washed with distilled water before electrochemical testing.

Electrolyte

The solutions employed were prepared using analytical grade chemicals and deionized water ($\rho = 18\text{ M}\Omega\text{ cm}$). Three

solutions were prepared, a reference 0.1 M NaOH solution and two more solutions with NaCl added to the blank solution to reach 0.1 M and 0.5 M NaCl.

The concentration range of inhibitor (plant extract) employed was varied from 50 to 500 ppm and the electrolyte used was 100 mL.

Electrochemical measurements

Open circuit potential measurements

A three-electrode cell assembly consisting of a mild steel coupon of 0.1 cm^2 nominal active surface embedded in a specimen holder was the working electrode (WE) and the only exposed area to the corrosive media the electrode was abraded with emery paper (grade 500–600–1200) on the test face, rinsed with distilled water and dried. A large area graphite sheet was the counter electrode (CE), and a saturated calomel electrode the reference electrode (RE). Before starting the experiments, the working electrode was immersed in test solution for 1 min at open circuit potential (OCP). The electrochemical cell contained 100 ml of electrolyte measurements were performed at 25, 30, 35, 40 and $45\text{ }^\circ\text{C}$.

Electrochemical impedance spectroscopy (EIS)

An Autolab® potentiostat PGSTAT 20 equipped with FRA32 module was employed for the electrochemical measurements. The data analysis was conducted using the dedicated Autolab® software that implements the fitting impedance utility developed by B. A. Boukamp.²¹ The impedance measurements were carried out at the open circuit potential (E_{OCP}) and FRA software. The alternating current frequency range was extended from 10 kHz to 0.01 Hz with a signal amplitude perturbation of 0.01 mV rms.

SEM analysis

Specific test coupons were exposed for 6 hours at $25\text{ }^\circ\text{C}$ and at $45\text{ }^\circ\text{C}$ in 100 ml of 0.1 M NaOH + 0.5 M NaCl having 100 ppm inhibitor, the optimal concentration of the inhibitor. After washing and drying, the specimens were examined for their structural and topographical features using a JEOL JSM-6510 S Scanning electron microscope (SEM).

FT-IR characterization

The pure aqueous and methanolic extracts and the scratched corrosion products formed on the mild steel surface were analyzed separately with the help of FT-IR (NICOLET FT-IR spectrometer Model no: 6700) spectra using the KBr pellet method.

CONCLUSIONS

In this paper, we demonstrated that aqueous extract of Prickly Pear gives an inhibition efficiency around 96.9% in NaOH (0.1 M) solution while the inhibition efficiency of methanol extract exceeded 88.3% in 0.1 M NaOH + 0.5 M NaCl solution, presenting a good inhibitor for steel corrosion. The impedance data was obtained via adsorption of the extract species on the C-steel surface. The inhibiting protection increases proportionally with the inhibitor concentration reached a maximum at 100 ppm. SEM reveals the

formation of a smooth surface on C-steel in the presence of prickly pear extract compounds probably due to the formation of an adsorptive film of electrostatic character. Besides, FTIR results indicate the presence of a uniform and dense adsorptive film over the C-steel surface, which efficiently inhibits the corrosion of c-steel. Those results were confirmed by the impedance study, which presented two phenomena included a charge-transfer and a passive layer.

REFERENCES

1. A. K. Singh, S. Mohapatra and B. Pani, *J. Ind. Eng. Chem.*, **2016**, *33*, 288-297; doi:10.1016/j.jiec.2015.10.014.
2. G. L. F. Mendonça, S. N. Costa, V. N. Freire, P. N. S. Casciano, A. N. Correia and P. de Lima-Neto, *Corros Sci.*, **2017**, *115*, 41-55; doi:10.1016/j.corsci.2016.11.012.
3. M. Prabaharan, S.-H. Kim, V. Hemapriya and I.-M. Chung, *J. Ind. Eng. Chem.*, **2016**, *37*, 47-56; doi:10.1016/j.jiec.2016.03.006.
4. S. Mo, H.-Q. Luo and N.-B. Li, *Chem Pap.*, **2016**, *70*, 1131-1143; doi:10.1515/chempap-2016-0055.
5. B. Guitián, X. R. Nóvoa and B. Puga, *Electrochim Acta.*, **2011**, *56*, 7772-7779; doi:10.1016/j.electacta.2011.03.055.
6. K. Cellat, F. Tezcan, B. Beyhan, G. Kardaş and H. Paksoy, *Constr. Build Mater.*, **2017**, *143*, 490-500; doi:10.1016/j.conbuildmat.2017.03.165.
7. H. Nahali, H. Ben Mansour, L. Dhouibi and H. Idrissi, *Constr. Build Mater.*, **2017**, *141*, 589-597; doi:10.1016/j.conbuildmat.2017.02.147.
8. H. Verbruggen, H. Terryn and I. De Graeve, *Constr. Build Mater.*, **2016**, *124*, 887-896; doi:10.1016/j.conbuildmat.2016.07.115.
9. P. B. Raja and M. G. Sethuraman, *Mater. Lett.*, **2008**, *62*, 113-116; doi:10.1016/j.matlet.2007.04.079.
10. G. Pena, C. M. Abreu and M. J. Crist, *J. Electroanal. Chem.*, **2004**, *572*, 335-345; doi:10.1016/j.jelechem.2004.01.015.
11. A.Y. El-Etre, M. Abdallah and Z. E. El-Tantawy, *Corrosion Sci.*, **2005**, *47*, 385-395; doi:10.1016/j.corsci.2004.06.006.
12. N. Etteyeb, L. Dhouibi, H. Takenouti, M. C. Alonso and E. Triki, *Electrochim. Acta*, **2007**, *52*, 7506-7512; doi:10.1016/j.electacta.2007.03.003.
13. V. K. Gouda, *Br. Corros. J.*, **1970**, *5*; doi.org/10.1179/000705970798324450.
14. L. Valek, S. Martinez, D. Mikulic and I. Brnardic, *Corrosion Sci.*, **2008**, *50*, 2705-2709; doi:10.1016/j.corsci.2008.06.018.
15. J. Hugo Cota-Sánchez, Chapter 28: "Nutritional Composition of the Prickly Pear (*Opuntia ficus-indica*) Fruit", in "Nutritional Composition of Fruit Cultivars", **2015**, p. 691-709; doi:10.1016/B978-0-12-408117-8.00028-3.
16. O. Khatabi, H. Hanine, D. Elothmani and A. Hasib, *Arab. J. Chem.*, **2016**, *9*, 278-281; doi:10.1016/j.arabjc.2011.04.001.
17. H. Ha and P. Felker, *J. Arid. Environ.*, **1997**, *36*, 133-148; doi:10.1006/jare.1996.0202.
18. H. N. le Houérou, *Options Méditerranéennes, Ser B.*, **2002**, *37*, 21-29.
19. J. C. Dubeux and U. Brazil, Use of Cactus for Livestock.
20. F. C. Stintzing and R. Carle, *Mol. Nutr. Food Res.*, **2005**, *49*, 175-194; doi:10.1002/mnfr.200400071.
21. B. A. Boukamp, *Solid State Ionics*, **1986**, *18-19*, 136-140. doi:10.1016/0167-2738(86)90100-1.
22. S. Joiret, M. Keddad, X. R. Nóvoa, M. C. Pérez, C. Rangel and H. Takenouti, *Cem. Concr. Compos.*, **2002**, *24*, 7-15. doi:10.1016/S0958-9465(01)00022-1.
23. M. Sánchez-Moreno, H. Takenouti, J. J. García-Jareño, F. Vicente and C. A. Alonso, *Electrochim. Acta*, **2009**, *54*, 7222-7226; doi:10.1016/j.electacta.2009.07.013.
24. C. M. Abreu, M. J. Cristóbal, R. Losada, X. R. Nóvoa, G. Pena and M. C. Pérez, *Electrochim. Acta*, **2006**, *51*, 1881-1890; doi:10.1016/j.electacta.2005.06.040.
25. M. Lebrini, G. Fontain, L. Gengembre, M. Traisnel, O. Lerasleand N. Genet, *Appl. Surf. Sci.*, **2008**, *254*, 6943-6947; doi:10.1016/j.apsusc.2008.04.112.
26. K. F. Khaled, *J. Electrochem. Soc.*, **2010**, *157*, 116; doi:10.1149/1.3274915.
27. L. J. Li, X. P. Zhang, J. L. Lei, J. X. He and S. T. Zhang, *Asian J. Chem.*, **2012**, *24*, 1649-1653.
28. F. Mansfeld, M. W. Kendigand S. Tsai, *Corrosion*, **1982**, *38*, 478-485; doi:10.5006/1.3577363.
29. H. Shih and F. A. Mansfeld, *Corros. Sci.*, **1989**, *29*, 1235-1240; doi:10.1016/0010-938X(89)90070-X.
30. S. Martinez, M. Metikoš-Huković, *J. Appl. Electrochem.*, **2003**, *33*, 1137-1142.
31. F. Bentiss, M. Lebrini, H. Vezin, F. Chai, M. Traisnel and M. Lagrené, *Corros. Sci.*, **2009**, *51*, 2165-2173; doi:10.1016/j.corsci.2009.05.049.
32. M. Behpour, S. M. Ghoreishi, N. Soltani, M. Salavati-Niasari, M. Hamadani and A. Gandomi, *Corros. Sci.*, **2008**, *50*, 2172-2181; doi:10.1016/j.corsci.2008.06.020.
33. M. Lagren, *Corros. Sci.*, **2002**, *44*, 573-588; doi:10.1016/S0010-938X(01)00075-0.
34. M. I. Awad, *J. Appl. Electrochem.*, **2006**, *36*, 1163-1168; doi:10.1007/s10800-006-9204-1.
35. E. E. Oguzie, Y. Li and F. H. Wang, *Electrochim. Acta.*, **2007**, *53*, 909-914; doi:10.1016/j.electacta.2007.07.076.
36. X.-H. Li, S.-D. Deng, H. Fu and G.-H. Mu, *J. Appl. Electrochem.*, **2009**, *39*, 1125-1135; doi:10.1007/s10800-008-9770-5.
37. S. Deng, X. Li and H. Fu, *Corros. Sci.*, **2011**, *53*, 760-768; doi:10.1016/j.corsci.2010.11.002.
38. Q. Qu, S. Jiang, L. Li, W. Bai and J. Zhou, *Corros. Sci.*, **2008**, *50*, 35-40; doi:10.1016/j.corsci.2007.06.008.